

# A New 3-D Assembly Approach For Nanoelectromechanical Switch Fabrication

Chen Yang

The State Key Laboratory of Robotics and Systems  
Harbin Institute of Technology  
150001 Harbin, P. R. China  
Email: yangchen.hope@yahoo.com.cn

Hui Xie

The State Key Laboratory of Robotics and Systems  
Harbin Institute of Technology  
150001 Harbin, P. R. China

Jihong Yan

The State Key Laboratory of Robotics and Systems  
Harbin Institute of Technology  
150001 Harbin, P. R. China

Jie Zhao

The State Key Laboratory of Robotics and Systems  
Harbin Institute of Technology  
150001 Harbin, P. R. China

**Abstract**—Achieving high-accuracy and repeatable fabrication of nanoelectromechanical switch is a grand challenge. In this paper, a new approach based on 3-D nanomanipulation has been proposed to integrate zinc oxide nanowire with lithographically patterned electrodes. Compared with other methods, a high level of manipulation accuracy can be reached without utilizing advanced lithographic tools. The device itself is actuated by electrostatic force and its physical model has also been developed for determining several key parameters. After the process of assembly, an *in situ* electrical characterization experiment is conducted. Experimental results illustrate the low pull-in voltages of the device combined with nearly zero current leakage, which are key parameters for being a good substitute of the CMOS devices in the future.

**Keywords**—nanoelectromechanical switch; 3-D nanoassembly; electrostatic force actuation ; electrical characterization

## I. INTRODUCTION

During the past several decades, the success of scaling technologies has brought complementary metal oxide semiconductor (CMOS) devices into the nanoscale level and therefore boosting its overall performance to a large degree [1]. However, further development of scaling down is still a grand challenge due to the intrinsic limitations of conventional CMOS device physics [2], [3], [4]. For the purpose of seeking an effective way to mitigate this issue thus exploring new opportunities for exponential development of future electronics [5], the nanoelectromechanical switches (NEMS), which possess several obvious merits such as nearly zero leakage current and high drive current, are viewed as good substitute of current CMOS devices [6].

From the point of fabrication, two main approaches including the top-down approach and the bottom-up approach have been conducted. In the top-down approach, nanostructures are typically fabricated by advanced lithographic and etching techniques, i.e. e-beam lithography [7]. As this classical approach is very closed to its physical limitation, the bottom-up approach, which constructs new types of nanostructures by

integrating materials obtained from growth techniques [8], has established itself as a promising way for achieving nano-electronic devices.

As one of the key issues in bottom-up fabrication process is how to position nanomaterials relative to other components efficiently, various approaches including scanning electron microscope (SEM) [9], [10], dielectrophoresis [11] and optical traps [12] have been proposed. Unlike approaches mentioned above, we propose a novel 3-D assembly strategy based on a dual-probe nanotweezer. In this strategy, Zinc oxide (ZnO) nanowire is picked up carefully and then released to a predetermined location. Generally speaking, our approach possesses three main advantages: 1) The manipulation process of nanowire has been conducted under the guide of atomic force microscopy (AFM) force sensing and image scan and therefore achieving a high level of manipulation accuracy. 2) Benefiting from the adoption of one dimensional nanomaterials, advanced etching techniques are not indispensable. 3) The *in situ* electrical measurement of fabricated NEMS could be easily performed by utilizing the conductive probes.

In this paper, the approach of fabricating a 2-terminal (2-T) NEMS is presented by using the 3-D assembly strategy mentioned above. Electrodes of NEMS can be obtained from conventional photolithography techniques. In our previous work [13], a dual-probe nanotweezer has been constructed and now used for integrating ZnO nanowire with electrodes. After the process of fabrication, the suspended structure of the NEMS has been formed and then procedures for achieving its volt-ampere characteristics will be started.

## II. MODELING AND DESIGN OF 2-T NEMS

### A. Principle of the 2-T NEMS

The 2-T NEMS is comprised of a ZnO nanowire which serves as a movable electrode and two fixed electrodes, as shown in Fig.1. When a potential difference is imposed between two parallel electrodes, the electrostatic force will be introduced

and attracts the ZnO nanowire down to the fixed electrode. Key parameters of the NEMS include suspended length of the nanowire ( $L$ ), gap between the nanowire and bottom electrode ( $h$ ) and pull-in voltage ( $V_i$ ). The relationship among these parameters will be shown in the physical model of 2-T NEMS and detailed as follows.

### B. Physical Model

As the diameter of the nanowire (chosen around 100nm) is much smaller compared with the dimensions of electrodes, interactions between them could be seen as a model of a finite

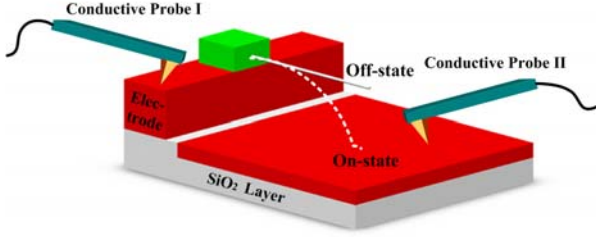


Figure 1. Schematic diagram of the 2-T NEMS, which consists of a suspended nanowire and a bottom electrode. The electromechanical force is introduced by imposing a voltage via conductive probe I and probe II.

wire versus an infinite plane. The potential  $U(x, y)$  of any point in the space is described as:

$$U(x, y) = \frac{\lambda}{4\pi\epsilon_0} \ln \left[ \frac{b-y+\sqrt{x^2+(y-b)^2+(z-h)^2}}{b-y+\sqrt{x^2+(y-b)^2+(z+h)^2}} \right] \frac{-y+\sqrt{x^2+y^2+(z+h)^2}}{-y+\sqrt{x^2+y^2+(z-h)^2}} \quad (1)$$

where  $\lambda = CV_i/L$ , represents the charge density per unit length of the nanowire,  $\epsilon_0$  is the dielectric constant in vacuum, equivalent capacitance  $C$  between nanowire and the fixed electrode can be obtained from [14]:

$$C = \frac{2\pi\epsilon_0 L}{\ln(2h/R)} \approx 2.0 \times 10^{-6} \text{ F} \quad (2)$$

Then the charge density  $\delta(x, y)$  on the surface of electrode can be determined from potential distribution above (as shown in Fig.2):

$$\delta(x, y) = -\epsilon_0 \frac{\partial U}{\partial z} \Big|_{z=0} = \frac{\lambda}{4\pi} \left[ \frac{2h}{(\sqrt{x^2+(y-b)^2+h^2})(b-y+\sqrt{x^2+(y-b)^2+h^2})} - \frac{2h}{(\sqrt{x^2+y^2+h^2})(-y+\sqrt{x^2+y^2+h^2})} \right] \quad (3)$$

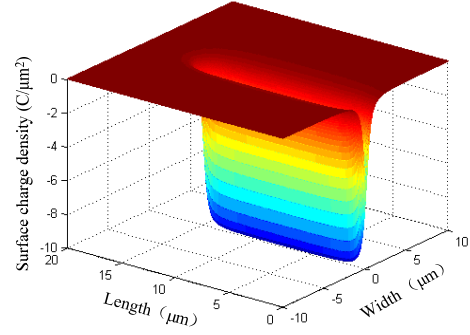


Figure 2. The charge density on the surface of bottom electrode, which indicates the charge density will be declined to almost zero if the distance away from the nanowire reaches to 10  $\mu\text{m}$  and then the effect of induced electric field can be omitted.

When applying a potential difference between the suspended nanowire and the bottom electrode, an electrostatic force is introduced and then used for actuating the NEMS. Apart from the electrostatic force, other short range forces such as the van der Waals force, may also attract the nanowire down to the fixed electrode. During the dynamic process of being turned on, a larger force is needed when ZnO nanowire starts to bend. A schematic illustration of physical model is shown in Fig.3.

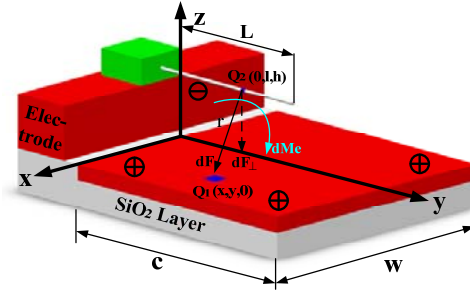


Figure 3. Physical model of 2-T NEMS, where an electrostatic force  $dF$  is applied between two points  $Q_1$  at  $(x, y, 0)$  and  $Q_2$  at  $(0, l, h)$ . The vertical component of  $dF$  will lead to a bending moment  $dMe$ .

The electrostatic force between infinitesimal element  $dl$  along the nanowire and  $ds$  on the electrode surface can be obtained by taking Coulomb's law:

$$dF = \frac{Q_1 Q_2}{4\pi\epsilon_0 r^2} \quad (4)$$

where  $Q_1 = \delta(x, y) dx dy$ ,  $Q_2 = CV dl_i / L$  are the electric charge of  $dl$  and  $ds$  respectively,  $r = \sqrt{x^2 + (y-l)^2 + h^2}$  represents the distance between them.

The bending moment as a whole caused by the electrostatic force can be achieved as:

$$Me = \frac{C^2 V_t^2 h}{16\pi^2 \epsilon_0 L} \int_{-w/2}^{w/2} \int_0^L \left[ \frac{2h}{(\sqrt{x^2 + (y-L)^2 + h^2})(L-y+\sqrt{x^2 + (y-L)^2 + h^2})} - \frac{2h}{(\sqrt{x^2 + y^2 + h^2})(-y+\sqrt{x^2 + y^2 + h^2})} \right] \cdot \frac{1}{r^3} dx dy dl \quad (5)$$

According to material mechanics, the corresponding bending moment caused by the elastic force of the nanowire is  $M = EI/\rho$ , where  $I = \pi d^4/64$  is the moment of inertia,  $\rho = (L^2 + h^2)/2h$  represents the curvature radius of bending nanowire.

### C. Analysis and Design of Key Parameters

According to Fig.2, dimensions of the electrode are chosen as: the width  $w = 20\mu\text{m}$  and the length  $c = 15\mu\text{m}$ . In the case of  $L = 15\mu\text{m}$ ,  $h = 0.4\mu\text{m}$  and  $V_t = 3.8\text{V}$ , the Young's Modulus of the ZnO nanowire can be determined as:

$$E = \frac{C^2 V_t^2 h r}{16\pi e_0 L^2 I} I_0 = 305.07 \text{ GPa} \quad (6)$$

This value is much larger than the published results from [15], [16], and [17], which indicates the key parameters mentioned above can be further optimized.

According to (5), the relationship between suspended length and the Young's modulus of the nanowire can be obtained. As the Young's modulus of the nanowire below 60GPa, the suspended length can be chosen in the range of 3-3.5  $\mu\text{m}$ .

Meanwhile, a negative correlation between the Young's modulus and the depth of the electrode is shown in Fig.4. A deeper gap will result in a larger elastic force of the nanowire, and therefore making the establishment of a contact with the fixed electrode more difficult. The threshold of Young's modulus is 60GPa which corresponds to a gap of 320nm. Consequently, the value of the gap can be chosen in the range of 300-350nm. Above all, the ranges of key parameters have been determined and will be further used in the process of photolithography.

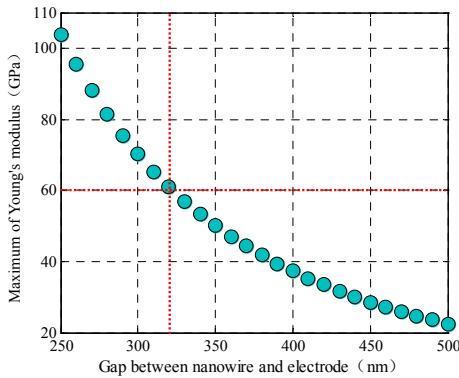


Figure 4. Negative correlation between the gap and Young's modulus, the threshold of Young's modulus corresponds to a 320nm-deep gap.

### D. Fabrication of Electrode

Electrodes of the NEMS are fabricated by using conventional photolithography techniques. The starting material of

the device is an n-type silicon (Si) wafer coated by a 700nm-thick silicon dioxide ( $\text{SiO}_2$ ) film for electrical isolation. Then a layer of photoresist is covered on the top of oxide coating and patterned to form chemical corrosion window. After the process of wet etching, the gap used for actuating nanowire has been formed with a height of 350nm. In the subsequent procedures, a 300nm-thick aluminum (Al) layer is deposited on the surface of oxide layer. The electrodes can be obtained eventually by removing undesired parts of metal layer through another standard lithography process.

## III. 3-D ASSEMBLY EXPERIMENT

### A. System Configuration of Dual-Probe Nanotweezer

In our previous work, a nanotweezer has been constructed and used for three-dimensional nanomanipulation. As shown in Fig.5, the system is comprised of an optical microscope and two sets of devices commonly used in conventional atomic force microscope. Every set of device contains a micro cantilever, a XYZ nanostage and an optical lever. The optical

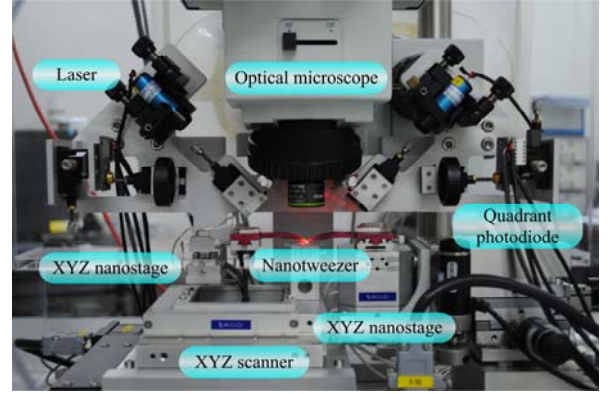


Figure 5. System configuration of dual-probe nanotweezer. The nanotweezer consists of two individually actuated cantilevers with protrudent tips. Probe I (on the right) serves a manipulation tool by pushing and pulling nanoobject while probe II acts as an imaging sensor to provide position information.

lever, detecting light deflection by a quadrant photodiode and several optical lenses, serves as a force sensor to monitor the actions of microcantilever during the process of nanomanipulation. During the process of 3-D manipulation, both of the two probes move toward the nanoobject, once a solid contact have been established between probe and nanoobject, the nano-tweezer is formed and subsequent steps of manipulation can be started.

### B. 3-D Assembly Protocol of the NEMS

Typically, the process of integrating ZnO nanowire with electrodes follows a scan-operation-scan cycle (several steps of 3-D nanoassembly and the final suspended structure are shown in Fig.6):

- Locating probes and nanowire. Initially, two probes are aligned above the centre of manipulation area and the first step is to establish a contact between probes and substrate (electrode). Subsequently, probe II is used to

scan manipulation area and therefore locations of nanowire and probe I can be determined.

- Building contact with the nanowire. As both of the two probes working in tapping mode, amplitude signals are helpful for contact detection. During the process of moving sample holder, when the voltage output of amplitude declines to zero, a solid contact has been established. By adjusting the locations of probes, a nanotweezer is able to be formed.
- Picking up the ZnO nanowire. After the process of clamping one end of the nanowire, the picking up step is able to be implemented by moving sample holder downward.
- Transporting and releasing nanowire. The nanotweezer transports clamped nanowire to the predetermined location by moving sample holder on the x, y direction. Meanwhile a displacement on the z direction is needed in order to realize release operation.
- Re-scanning and determining displacements for next nanomanipulation.

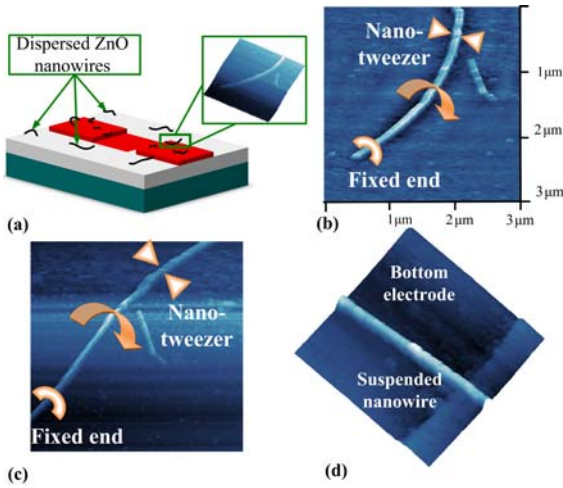


Figure 6. (a) Choosing a nanowire to be manipulated by scanning the surface of electrode. (b) A scanned image before manipulation, in which the position of nanotweezer and transportation direction has been shown. (c) The result of first nanomanipulation. (d) A suspended nanowire is formed over the bottom electrode.

### C. Analysis of Grasping Force

Fig.7 illustrates the normal voltage output of one probe during process of pick-and-place. The operation starts from point A, where a solid contact has been established. When sample holder moving downward, the voltage output decreases sharply due to the adhesion force between probe and substrate, namely, snap in appears. After point B, another sudden increase occurs as the sample holder continues its movement. The reason of this change is that the elastic force of cantilever has become large enough and can be used for balancing adhesion force. This pull-off process lasts from point B to point C. Subsequent procedures of pick-up keep stable until releasing process starts from point D. Actually, there is no

sudden change appears in releasing operation except a mild snap in just before releasing process is completed.

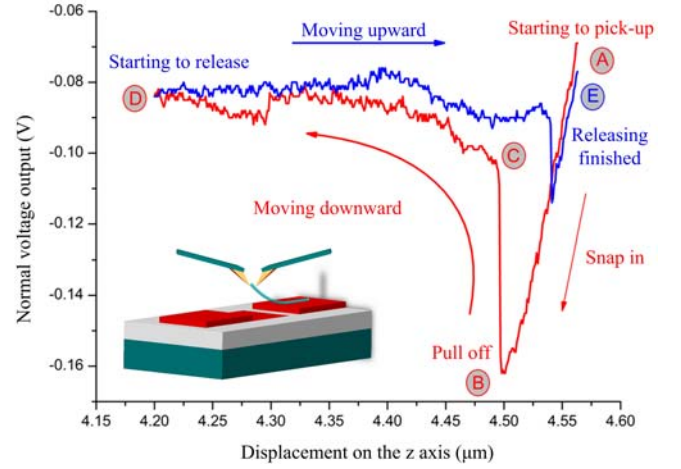


Figure 7. The applied force of one probe during the manipulation process of pick-and-place.

According to the voltage output curve combined with normal stiffness of the probe, real forces applied on cantilever are able to be obtained. In this study, the stiffness of the probe is 2.8N/m with a resonant frequency of 70.37 KHz (Nanosensors, ATEC-FM-50).

During the pickup, interactive forces between probes and nanowire include clamping forces  $F_{n1}$ ,  $F_{n2}$ ; adhesion forces  $F_{s1}$ ,  $F_{s2}$  on the interface; friction forces  $F_{f1}$ ,  $F_{f2}$  and adsorption force  $F_a$ , as shown in Fig.8. Equilibrium equation can be deduced as:

$$\begin{cases} F_x = (F_{n1} - F_{s1}) \sin \phi - F_{f1} \cos \phi \\ F_y = (F_{n1} - F_{s1}) \cos \phi + F_{f1} \sin \phi = \frac{1}{2} F_a \\ F_{f1} = \tau S = \tau \pi \left[ \frac{3(F_{n1} + F_{s1}) \text{Re}}{4E^*} \right]^{\frac{2}{3}} \cdot F_1(e)^2 \\ F_s = \frac{4\pi R_e \Delta W}{\sin \theta} \end{cases} \quad (7)$$

where  $R_e = \frac{R_1 R_2}{R_1 + R_2}$ ,  $E^* = \left( \frac{1-\gamma_1^2}{E_1} + \frac{1-\gamma_2^2}{E_2} \right)^{-1}$  represent equivalent

radius and stiffness.  $R_i$ ,  $E_i$  and  $\gamma_i$  ( $i=1,2$ ) are radius, Young's modulus and Poisson's ratio of tip and nanowire (subscript 1 and 2 correspond to tip and nanowire respectively),  $\phi = 68^\circ$  is the tilted angle of the tip,  $\Delta W$  stands for surface energy.  $F_1(e)$  can be deduced from complete elliptic integrals with a value of  $F_1(e) = 0.7769$ . Other parameters used in (7) have been shown in TABLE I. Based on these parameters, equivalent radius  $R_s = 8.33 \times 10^{-9}$  m, equivalent stiffness  $E^* = 44.9$  GPa, adhesion force  $F_{s1} = 146.53$  nN. The curve shown in Fig.7 indicates that the peak of grasping force appears at point C (with a voltage output of 105mV) which corresponds to a

pick-up force of 305.91nN. Consequently, the clamping force  $F_n = 917.5\text{nN}$ , the friction force  $F_f = 73.6\text{nN}$  and the adhesion force  $F_a = 611.82\text{nN}$  can be finally calculated.

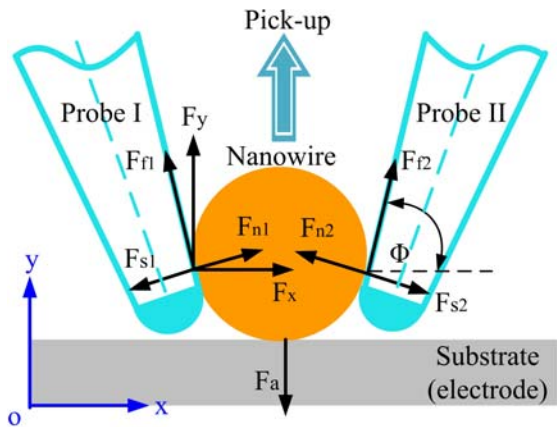


Figure 8. A schematic of interactive forces analysis which includes clamping forces, friction forces, adsorption forces as well as adhesion forces from two contact interface.

TABLE I. KEY PARAMETERS USED IN INTEACTIVE FORCES ANALYSIS

	<i>Probe</i>	<i>Nanowire</i>	<i>Substrate</i>
Material	Silicon	Zinc oxide	Silicon oxide
Radius (R)	10nm	50nm	$\rightarrow \infty$
Surface energy ( $\Delta W$ )	1.4 J/m <sup>2</sup>	1.42 J/m <sup>2</sup>	1.14 J/m <sup>2</sup>
Young's modulus (E)	160 GPa	60 GPa	70.3 GPa
Poisson's ratio ( $\gamma$ )	0.17	0.165	0.33

#### IV. ELECTRICAL CHARACTERIZATION OF THE NEMS

As shown in Fig.1, testing process for obtaining volt-ampere characteristics of fabricated NEMS is implemented by using conductive probes (Nanosensors, PPP-EFM). In this scheme, electrical measurement can be easily conducted benefiting from two probes we have used, which will impose potential difference directly without complicated procedures.

The results of electrical testing have been shown in Fig.9, which plot the potential difference required to turn on the NEMS. According to the illustration, the switch still remains off until the voltage reaches its threshold, namely, pull-in voltage. Then the electrostatic force bends the nanowire to establish a contact with bottom metal electrode. Procedures of regulating external voltage have been repeated for three times and corresponding pull-in voltages are 5.80V, 7.04V and 6.52V respectively. In addition, the off-state current has also been obtained with a value less than 30nA, therefore demonstrating the switch's performance of nearly zero current leakage.

At the same time, the on-state current is relatively low due to a large contact resistance between the nanowire and metal electrode. Therefore, more efforts are still necessary to enhance the on/off current ratio to a higher level.

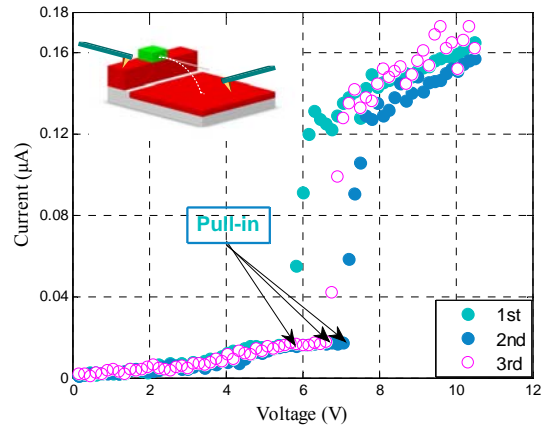


Figure 9. Three V-I curves are obtained from electrical characterization, showing different pull-in voltages in three consecutive tests between 5V and 7V.

#### V. CONCLUSION

In summary, we have presented a new approach for fabricating nanoelectromechanical switch. Several conclusions based on this method can be drawn as follows. (1) The physical model of an electrostatic force actuated 2-T NEMS has been constructed and used for designing its key parameters. (2) The elasticity mechanics model for analyzing interactive forces between probes and nanowire is also developed. (3) By using conductive probes, electrical testing process is able to be implemented, since the external voltage has been introduced and imposed on two parallel electrodes. Experimental results exhibit a promising future of the fabricated NEMS for its nearly no power consumption in the off state combined with a mild pull-in voltage.

#### ACKNOWLEDGMENT

This work was supported in part by the National Natural Foundation of China under grant 90923041 and 51175130, the State Key Laboratory of Robotics and Systems under grant SKLRS201001D and SKLRS201001B, the Ministry of Education Key Laboratory of Microsystems and Microstructure Manufacturing under grant.

#### REFERENCES

- [1] A.Khakifirooz and D.A.Antoniadis, "MOSFET performance scaling-part I: historical trends," IEEE. Trans. Electron Devices, vol.55, pp. 1391-1400, June 2008.
- [2] E.J.Nowak, "Maintaing the benefits of CMOS scaling when bogs down," IBM. J. Research and Development, vol. 46, pp. 169-180, March 2002.
- [3] S.Borkar, "Design challenges of technology scaling," Micro. vol.19, pp.23-29, Jul-Aug 1999.
- [4] S.G.Narendra and A.Chandrakasan, Leakage in Nanometer CMOS Technologies. Springer, Nov.2005.
- [5] L.L.Chang, Y.K.Choi, J.Kedzierski, N.Lindert, P.Q.Xuan, J.Bokor, C.M.Hu, and T.J.King, "Moore's law lives on-Ultra-thin body SOI and FinFET CMOS transistors look to continue moore's law for many years to come," IEEE. Trans. Circuits Devices, vol.19, pp.35-42, 2003.
- [6] S.N.Cha, J.E.Jang, Y.Choi, G.A.Amaratunga and D.J.Kang, "Fabrication of a nanoelectromechanical switch using a suspended carbon nanotube," Appl.Phys.Lett, vol.86, pp. 83105-83105-3, Feb 2005.

- [7] C.Vieu, F.Carcenac, A.Lebie, L.Couraud and H.Launois. "Electron beam lithography: resolution limits and applications," *Applied surface science*, vol.164, pp.111-117, Sep 2000.
- [8] Y.Huang, X.Duan, Y.Cui, L.J.Laudon and C.Lieber, "Logic gates and computation from assembled nanowire building blocks" *Science*, vol.294, pp. 1313–1317, Nov 2001.
- [9] S.Fahlbusch, S.Mazerolle, J.M.Breguet, A.Steinecker, J.Agnus, and J.Michler. "Nanomanipulation in a scanning electron microscope," *J. Materials Processing Technology*, vol.167, pp. 371–382, 2005.
- [10] M.Noyong, K.Blech, A.Ronsenberger, V.Klocke and U.Simon, "*In situ* nanomanipulation system for electrical measurement in SEM," *Meas. Sci. Technol*, No.12, Sep 2007.
- [11] K.Carmen, M.Fung, T.Victor, S.Wong, H.Rosa, M.Chan, J.Wen, "Dielectrophoretic batch fabrication of bundled carbon nanotube thermal sensors," *IEEE. Trans. Electron Devices*, vol.55, pp. 1391–1400, June 2008.
- [12] R.Agarwal, K.Ladavac, Y.Roichman, G.H.Yu, C.M.Lieber and G.Grier, "Manipulation and assembly of nanowires with holographic optical traps," *Optics.Expr*, vol.13, pp. 8906–8912, 2005.
- [13] H.Xie, D.S.Haliyo and Stéphane Régnier, "A versatile atomic force microscope for three-dimensional nanomanipulation and nanoassembly," *Nanotechnology*, vol.20, no.21, May 2009.
- [14] O.Wunnicke, "Gate capacitance of back-gated nanowire field-effect transistors," *Appl. Phys. Lett*, vol.89, pp. 83102–83102-3, Aug 2006.
- [15] J.Song, X.Wang, E.Riedo and Z.L.Wang, "Elastic property of vertically aligned nanowires," *Nano.Lett*, vol.5, pp. 1954–1958, Sep 2005.
- [16] A.V.Desai and M.A.Haque, "Mechanical properties of ZnO nanowires," *Sens.Actua*, vol.134, pp.169–176, Feb 2007.
- [17] Y.Huang, X.Bai and Y.Zhang, "In situ mechanical properties of individual ZnO nanowires and the mass measurement of nanoparticles," *J. Phys.:Condens.Matter*, vol.18, pp. 179–184, June 2006.